ELSEVIER

The Journal of Heart and Lung Transplantation
http://www.jhltonline.org

ORIGINAL TRANSLATIONAL SCIENCE

Molecular states associated with dysfunction and graft loss in heart transplants

Philip F. Halloran, MD, PhD,[a] Katelynn Madill-Thomsen, PhD,[a] Martina Mackova, PhD,[a] Arezu Z. Aliabadi-Zuckermann, MD,[b] Martin Cadeiras, MD,[c] Marisa G. Crespo-Leiro, MD, PhD,[d] Eugene C. Depasquale, MD,[c] Mario Deng, MD,[c] Johannes Gökler, MD,[b] Shelley A. Hall, MD,[e] Daniel H. Kim, MD,[a] Jon Kobashigawa, MD,[f] Peter Macdonald, MD, PhD,[g] Luciano Potena, MD, PhD,[h] Keyur Shah, MD,[i] Josef Stehlik, MD, MPH,[j] Andreas Zuckermann, MD,[b] and Jeff Reeve, PhD[a]

From the [a]Department of Medicine, University of Alberta, Edmonton, Alberta, Canada; [b]Department of Cardiac Surgery, Medical University of Vienna, Vienna, Austria; [c]Ronald Reagan UCLA Medical Center, Los Angeles, California; [d]Complexo Hospitalario Universitario A Coruña, A Coruña, Spain; [e]Baylor Scott & White Health, Dallas, Texas; [f]Cedars-Sinai Medical Center, Los Angeles, California; [g]The Victor Chang Cardiac Research Institute, Sydney, Australia; [h]Heart Failure and Transplant Unit, IRCCS Azienda Ospedaliero-Universitaria di Bologna, Bologna, Italy; [i]Department of Cardiology, Virginia Commonwealth University, Richmond, Virginia; and the [j]Department of Medicine, University of Utah, Salt Lake City, Utah.

KEYWORDS:
heart transplant;
endomyocardial biopsy;
gene expression;
heart transplant survival;
left ventricular ejection fraction

BACKGROUND: We explored the changes in gene expression correlating with dysfunction and graft failure in endomyocardial biopsies.

METHODS: Genome-wide microarrays (19,462 genes) were used to define mRNA changes correlating with dysfunction (left ventricular ejection fraction [LVEF] ≤ 55) and risk of graft loss within 3 years postbiopsy. LVEF data was available for 1,013 biopsies and survival data for 779 patients (74 losses). Molecular classifiers were built for predicting dysfunction (LVEF ≤ 55) and postbiopsy 3-year survival.

RESULTS: Dysfunction is correlated with dedifferentiation—decreased expression of normal heart transcripts, for example, solute carriers, along with increased expression of inflammation genes. Many genes with reduced expression in dysfunction were matrix genes such as fibulin 1 and decorin. Gene ontology (GO) categories suggested matrix remodeling and inflammation, not rejection.

Genes associated with the risk of failure postbiopsy overlapped dysfunction genes but also included genes affecting microcirculation, for example, arginase 2, which reduces NO production, and endothelin 1. GO terms also reflected increased glycolysis and response to hypoxia, but decreased VEGF and angiogenesis pathways. T cell-mediated rejection was associated with reduced survival and antibody-mediated rejection with relatively good survival, but the main determinants of survival were features of parenchymal injury.

Both dysfunction and graft loss were correlated with increased biopsy expression of BNP (gene *NPPB*).

Survival probability classifiers divided hearts into risk quintiles, with actuarial 3-year postbiopsy survival > 95% for the highest versus 50% for the lowest.

Reprint requests: Philip F. Halloran, MD, PhD, Alberta Transplant Applied Genomics Centre, #250 Heritage Medical Research Centre, University of Alberta, Edmonton AB T6G 2S2, Canada. Telephone: 780-492-6160. Fax: 780-407-7450.
E-mail address: phallora@ualberta.ca.

https://doi.org/10.1016/j.healun.2023.11.013

CONCLUSIONS: Dysfunction in transplanted hearts reflects dedifferentiation, decreased matrix genes, injury, and inflammation. The risk of short-term loss includes these changes but is also associated with microcirculation abnormalities, glycolysis, and response to hypoxia.
J Heart Lung Transplant xxxx;xxx:xxx–xxx

Despite the success of heart transplantation, heart transplants often experience suboptimal outcomes. Many late hearts have impaired function, including diastolic dysfunction with preserved ejection fraction.[1] Survival is currently estimated to be at about 90% at 1 year, 80% at 5 years, and 50% at 10 years post-transplant.[2,3] A recent review of survival predictive models found insufficient data to recommend the use of one risk model over the others for the prediction of post-heart transplant outcomes.[4]

Genome-wide measurement of gene expression in the biopsy offers an opportunity to explore the mechanisms associated with dysfunction and failure. The Molecular Microscope Diagnostic System (MMDx)[5-11] (reviewed recently[6]) measures the expression of 19,462 genes using classifiers and archetypal analysis to identify rejection and injury phenotypes.[12] MMDx first analyzed T cell-mediated rejection (TCMR) and antibody-mediated rejection (ABMR) based on expression of rejection-associated transcripts (RATs)[10,13,14] and later characterized transcripts associated with parenchymal injury[12,15] and related rejection to injury and risk of graft failure.[16] TCMR and injury scores were associated with increased rates of graft loss whereas ABMR scores predicted relatively good short-term survival.[17]

The present study directly explored the molecular basis of heart dysfunction and risk of failure, exploring the changes in gene expression and pathways that correlate with left ventricular ejection fraction (LVEF) ≤ 55 at the time of biopsy and with risk of failure 3 years postbiopsy.

For a glossary of abbreviations, see Table S1.

Materials and methods

Population

MMDx assessments were available for 3,230 biopsies, including 1,641 INTERHEART biopsies and 1,589 service biopsies from the Kashi Clinical Laboratories (Figure 1). INTERHEART biopsies (ClinicalTrials.gov #NCT02670408) included biopsies from consenting patients at 10 centers (Table S2). The combined set of INTERHEART and service biopsies permitted an increase in the sample size to update all the machine learning algorithms and to generate a new MMDx-Heart report, which will be published separately (in preparation). For the present paper, although the service biopsies had minimal phenotype data, the combined INTERHEART and service biopsy sets were used to analyze the classifier-gene set correlations (see Results).

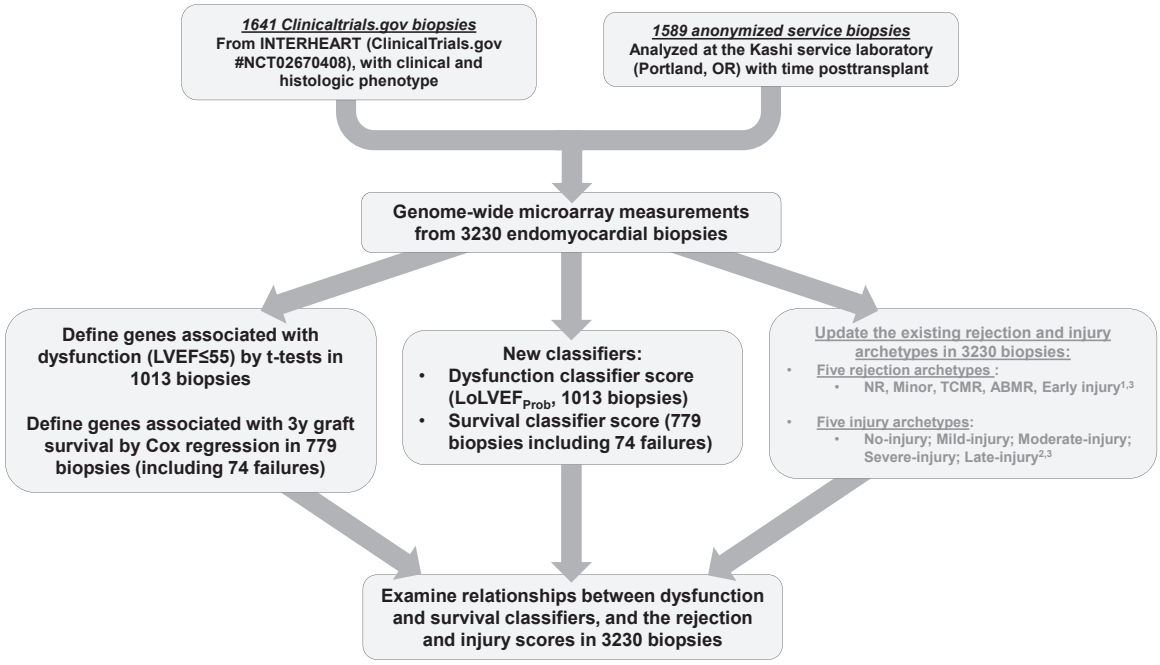

Figure 1 Study design. A flowchart describes how the molecular diagnostic classes were developed. The genes and pathways associated with dysfunction and survival were defined, dysfunction and survival classifiers were developed, and the relationship of the rejection and injury archetypes and other gene sets to the survival and injury classifiers were mapped. ABMR, antibody-mediated rejection; LVEF, left ventricular ejection fraction; NR, no-rejection; TCMR, T cell-mediated rejection.

Table 1 Biopsy Characteristics and Patient Demographics ($N = 3,230$)

Biopsy characteristics	All biopsies $N = 3,230$
Days to biopsy posttransplant (TxBx)	
Mean	1,181
Median (range)	350 (1, 11,007)
Days to most recent follow-up after biopsy	
Mean	610
Median (range)	313 (1, 3,854)
Indication for biopsy	
Clinical including follow-up (% of known)	259 (18.5)
Protocol biopsy (% of known)	1,142 (81.5)
Not stated (% of total)	1,829 (56.6)
Patient demographics	All patients $N = 1,091$
Mean patient age at transplant (range)	49.6 (2, 80)
Age at transplant > 65 years (%)	110 (10.1)
Mean donor age (range)	39.8 (6, 71)
Patient sex	
Male (% of known)	700 (66.1)
Female (% of known)	359 (33.9)
Unknown	32 (2,171 including the service laboratory biopsies)
Donor sex	
Male (% of known)	521 (65.5)
Female (% of known)	275 (34.5)
Not available (% of total)	296 or 2,434
Patient had a previous failed heart transplant	*24/670 with data available (3.6%)
Heart status at last follow-up	
Alive at last follow-up (% of known)	806 (90.6)
Deceased (% of known)	84 (9.4)
Not available (% of total)	202 (18.5)
Primary disease[a]	
Other cardiomyopathies	509 (65%)
Congenital heart defect (% of known)	39 (5%)
Coronary artery disease (% of known)	86 (11%)
Other (% of known)	145 (19%)
Not available (% of total)	312

[a]Some patients received more than 1 primary diagnosis.

Of patients with available patient identifier information ($N = 2,054$ from the INTERHEART study and from the service laboratory), 566 had repeat biopsies submitted to MMDx-Heart for analysis. Twenty transplants were noted as retransplant in this population. However, we note that this information is not always transmitted from the centers, and thus may underrepresent the number of retransplants present.

The demographics (Table 1) and case mix (Table S3) were similar to previous analyses.[17]

Microarray analysis

Biopsies were submitted to the study as 1 to 2 pieces. Extracted total RNA was labeled and hybridized to PrimeView microarrays (Applied Biosystems), as previously described.[7,11,15,16,18,19] CEL files are available on the Gene Expression Omnibus website (GSE150059). Biopsy processing was identical between the research and service laboratory.

Pathogenesis-based transcript sets (PBTs)

PBTs (Table S4) were previously annotated.[20] PBT scores are mean fold changes compared to controls (371 biopsies with no rejection and > 30 days post-transplant), calculated using the original $\log_2$ raw data.

Dysfunction (LVEF ≤ 55) classifier

The dysfunction classifier score ($\text{LoLVEF}_{\text{Prob}}$) was developed as the median score from 12 different machine learning methods, as previously described.[7] All scores in this paper are from the left-out folds in 10-fold cross-validation. Our goal was to predict any-cause low LVEF; therefore, we did not exclude samples with rejection from the classifier development stage.

The dysfunction classifier is not meant to predict clinically measured LVEF per se, but to identify patterns of gene expression characteristic of heart transplants with low LVEF (≤55). In INTERHEART, $N = 1,013$ biopsies had recorded LVEF values: 214 with LVEF ≤ 55, 799 with LVEF > 55.

Survival analysis

Analyses were based on death-censored graft survival, usually to 3-years postbiopsy. Patients surviving longer were censored at 3 years. Only biopsies with a valid follow-up status and follow-up time > 0 days were included, based on 1 random biopsy per transplant, leaving 779 biopsies from the original 1,181 eligible, with 74/779 failing before 3 years postbiopsy.

Random forest (RF) analyses for 3-year survival were performed using the "randomForestSRC" package in R.[21] Inputs were chosen based on our prior experience in other transplanted organs—largely kidney biopsies. In total, 33 variables were used for the full model including updated rejection and injury archetypal scores previously published[12,19]:

- Five injury archetype scores (No Injury, Severe-Recent, Late Atrophy-Fibrosis, Moderate-Recent, Mild-Recent)
- Three injury principal component (PC) scores (injury PC1, PC2, PC3).
- Five rejection archetype scores—No Rejection (NR), TCMR, Early injury, ABMR, and Minor rejection
- Three rejection PCs (rejection PC1, PC2, PC3)
- One classifier: $\text{LoLVEF}_{\text{Prob}}$ (this classifier is trained on the LVEF values recorded in the population: 214 with LVEF ≤ 55, 799 with LVEF > 55.)
- TxBx (time of biopsy posttransplant in days)
- Biopsy indication status (one random biopsy per patient: 156 for cause, 588 protocols, 35 missing but imputed within the RFs)
- Fourteen transcript set (PBT) scores: mast cell transcripts (MCAT),[22] IRRAT30,[23] IRITD3,[24] QCMAT,[25] AMAT1,[25] DSAST,[26] immunoglobulin transcripts,[27] HT1,[12,14] HT2,[12,14] NKB,[28] GRIT3,[13,29] ABMR-RAT,[10,13] TCMR-RAT,[10] and Rejection-RAT.[10]

All-cause LVEF was used for training the $\text{LoLVEF}_{\text{Prob}}$ classifier, and biopsies were not removed unless LVEF data was unavailable. Other abnormalities such as restrictive allograft failure

and diastolic dysfunction not captured by a decreased LVEF were not a focus of these analyses, but will be included in future studies.

A truncated RF survival model was used for all final analyses, selected by a minimal depth method using the "var.select" function from the "randomForestSRC" package.[21] Error rates are calculated in out-of-bag (OOB) biopsies from bootstrapping, analogous to test set statistics calculated in cross-validation.

We also predicted survival using cv.glmnet from the R glmnet package,[30] a regression method designed to combine automatic feature selection with prediction; 12,500 interquartile range-filtered probe sets were used as input (after standardization), and alpha set to 1.0 for lasso regression. In the full model (using all 779 biopsies), 77 probe sets were selected.

For both the RF and glmnet survival classifiers, 100 bootstraps were performed. In each bootstrap, the 779 biopsies were sampled 779 times at random, with replacement. Therefore, in any given bootstrap, a biopsy may be present 0, 1, 2, 3, etc. times. On average, ~37% of the biopsies ($N \approx 287$) are present 0 times—these, the OOB sample, become the test set for that bootstrap. The remaining ~492 constitute that bootstrap sample's training set. Classifiers were built in the training set, and survival predictions were made for the test set. Survival probability scores for each biopsy were averaged over the ~37/100 bootstrap iterations in which that biopsy was in a test set. The final survival probability was then calculated as the mean of the RF and glmnet probabilities, each of which used the above bootstrapping procedure. The C-statistic was calculated using this final set of 779 averaged test set probabilities.

Differential gene expression

The Bayesian *t*-test in R's "limma" package[31] was used to find the genes most differentially expressed between high (> 55) and low (≤55) LVEF biopsies. Gene expression changes correlating with survival were analyzed using univariate Cox regression using the "coxph" function from the R "survival" package.[32] All 49,495 probe sets on the array were assessed and selected by *p*-value.

Results

Population

The median time posttransplant was 349 days (range 1-11,007 days, Table 1). Of 1,641 INTERHEART biopsies, 259 biopsies were for indications (including follow-up) and 1,142 by protocol. As expected, dysfunction and failure were more frequent in indication biopsies (Table S5).

Gene expression changes associated with dysfunction (LVEF ≤ 55)

(The choice of LVEF ≤ 55 as the definition of dysfunction is elaborated in discussion.)

The top 20 dysfunction-associated genes (by *t*-test *p*-value)—16 decreased and 4 increased—are shown in Table 2. None of the top 20 genes were strongly related to rejection. The 16 top genes with decreased expression in hearts with dysfunction (LVEF ≤ 55) included many related to matrix, for example, *FBLN1*, *ADAMTSL3*, *PTN*, and *DCN*. Four genes with increased expression with dysfunction included 2 related to macrophages (*IGFBP2 and PTPN1*) and 2 expressed in cardiomyocytes (*RCAN1*, *ENO2*). *RCAN1* is the regulator of calcineurin 1. *ENO2* is involved in glycolysis.

Table 2 Top 20 Dysfunction Genes Associated With LVEF ≤ 55 Versus > 55 (by *P*-Value; $N = 1,013$)[1]

Gene Symbol	t	P Value	Adjusted P Value	Gene	PBT	Mean expression in biopsies	
						Low LVEF (≤55)	High LVEF (>55)
DENND2A	11.82	2.7E-30	1.3E-25	DENN/MADD domain containing 2A		107	134
FBLN1	10.21	2.4E-23	5.9E-19	fibulin 1		282	492
ADAMTSL3	10.12	5.5E-23	9.0E-19	ADAMTS like 3		94	133
ABCA8	10.04	1.1E-22	1.3E-18	ATP binding cassette subfamily A member 8	HT1	324	515
DCN	9.90	3.9E-22	2.9E-18	decorin	IRITD5	2629	4525
AMOT	9.83	7.3E-22	4.5E-18	angiomotin		89	127
FEZ1	9.64	4.2E-21	2.1E-17	fasciculation and elongation protein zeta 1	HT2	333	428
ABCA9	9.55	9.2E-21	3.8E-17	ATP binding cassette subfamily A member 9		157	260
PRTFDC1	9.52	1.2E-20	4.7E-17	phosphoribosyl transferase domain containing 1		79	101
PTPN1	-9.32	7.2E-20	2.2E-16	protein tyrosine phosphatase, non-receptor type 1	cIRIT,HT1	627	541
NEGR1	9.27	1.1E-19	3.2E-16	neuronal growth regulator 1		94	142
IGFBP2	-9.25	1.3E-19	3.6E-16	insulin like growth factor binding protein 2		1139	682
ENO2	-9.20	1.9E-19	5.0E-16	enolase 2 (gamma, neuronal)		185	152
RCAN1	-9.20	2.0E-19	5.0E-16	regulator of calcineurin 1	cIRIT	927	723
PHACTR3	9.15	3.0E-19	7.1E-16	phosphatase and actin regulator 3		58	84
DLK1	9.09	5.0E-19	1.1E-15	delta-like 1 homolog (Drosophila)		178	442
SCN4B	9.06	6.8E-19	1.5E-15	sodium channel, voltage gated, type IV beta subunit		124	166
EGFLAM	9.04	8.0E-19	1.7E-15	EGF-like, fibronectin type III and laminin G domains	HT1,IRITD5	125	151
PTN	8.97	1.4E-18	2.9E-15	Pleiotrophin		359	567
ABCA6	8.92	2.1E-18	3.8E-15	ATP binding cassette subfamily A member 6		183	247
Selected relevant gene not present in the top 20							
NPPB	-4.90	1.1E-06	1.7E-05	natriuretic peptide B	"NPB"	2620	1298

1.Grey shading indicates transcripts increased in hearts with dysfunction.
Abbreviations: IRITD5 - injury-repair induced transcripts day 5, cIRIT- cardiac injury and repair transcripts, ENDAT – endothelial transcripts, HTs – heart normal transcripts

Table 3 GO Terms for Top 200 Genes Decreased in Hearts With Dysfunction (1,013 EMBs)

ONTOLOGY[1]	ID	Description[2]	P value	Q value	Gene ID[3]	Count
CC	GO:00 62023	collagen-containing extracellular matrix	4.8E-12	1.1E-09	***FBLN1/DCN/EGFLAM***/VIT/LAMA4/OGN/AGT/DPT/COL6A6/FREM1/TNXA/CDON/LAMC1/COL15A1/FBLN5/LUM/PCSK6/WNT5A/MATN2/GPC4/PCOLCE/ITIH5/LTBP4/PODN	13
MF	GO:0PTN005201	extracellular matrix structural constituent	1.6E-10	5.3E-08	***FBLN1/DCN***/LAMA4/OGN/DPT/COL6A6/LAMC1/COL15A1/FBLN5/LUM/MATN2/ANOS1/PCOLCE/LTBP4/PODN	13
BP	GO:0030198	extracellular matrix organization	2.8E-07	2.6E-04	***FBLN1/ADAMTSL3/EGFLAM***/VIT/TLL2/AGT/PDGFRA/DPT/COL6A6/TNXA/LAMC1/COL15A1/FBLN5/LUM/DDR2	13
BP	GO:0043062	extracellular structure organization	2.9E-07	2.6E-04	***FBLN1/ADAMTSL3/EGFLAM***/VIT/TLL2/AGT/PDGFRA/DPT/COL6A6/TNXA/LAMC1/COL15A1/FBLN5/LUM/DDR2	4
BP	GO:0045229	external encapsulating structure organization	3.2E-07	2.6E-04	***FBLN1/ADAMTSL3/EGFLAM***/VIT/TLL2/AGT/PDGFRA/DPT/COL6A6/TNXA/LAMC1/COL15A1/FBLN5/LUM/DDR2	7
MF	GO:0015399	primary active transmembrane transporter activity	4.7E-06	7.9E-04	***ABCA8/ABCA9/ABCA6***/ABCA10/ABCC9/ABCD2/CYC1/CYBRD1/NDUFS2/NDUFB10	8
MF	GO:0140359	ABC-type transporter activity	8.2E-06	9.2E-04	***ABCA8/ABCA9/ABCA6***/ABCA10/ABCC9/ABCD2	6
BP	GO:2000027	regulation of animal organ morphogenesis	3.4E-05	2.1E-02	AGT/AR/WNT5A/GPC4/FGF7/ANKRD6/LGR4/APCDD1	4
MF	GO:0030021	extracellular matrix structural constituent conferring compression resistance	5.8E-05	4.9E-03	***DCN***/OGN/LUM/PODN	4
BP	GO:0060571	morphogenesis of an epithelial fold	6.2E-05	2.7E-02	BMP5/AR/EGFR/WNT5A	3
BP	GO:0030539	male genitalia development	7.4E-05	2.7E-02	PDGFRA/BMP5/AR/LGR4	3
BP	GO:0048806	genitalia development	7.6E-05	2.7E-02	PDGFRA/BMP5/AR/WNT5A/LGR4	4
BP	GO:0048146	positive regulation of fibroblast proliferation	9.3E-05	2.8E-02	AGT/PDGFRA/EGFR/WNT5A/DDR2	9
MF	GO:0005539	glycosaminoglycan binding	1.1E-04	6.9E-03	***DCN/EGFLAM/PTN***/VIT/PCSK6/ANOS1/PCOLCE/FGF7/ LTBP4/SLIT2	5
BP	GO:0048145	regulation of fibroblast proliferation	1.1E-04	2.8E-02	AGT/PDGFRA/EGFR/WNT5A/DDR2/DACH1	9
BP	GO:0060688	regulation of morphogenesis of a branching structure	1.3E-04	2.8E-02	AGT/AR/WNT5A/FGF7/LGR4	20
BP	GO:0048144	fibroblast proliferation	1.3E-04	2.8E-02	AGT/PDGFRA/EGFR/WNT5A/DDR2/DACH1	6
MF	GO:0019199	transmembrane receptor protein kinase activity	1.3E-04	6.9E-03	PDGFRA/EPHA3/EGFR/DDR2/LTBP4/PDGFRL	5
MF	GO:0051287	NAD binding	1.4E-04	6.9E-03	IDH3B/RNLS/SIRT3/NUDT6/NDUFS2	2
BP	GO:0050679	positive regulation of epithelial cell proliferation	2.0E-04	4.2E-02	***PTN***/LAMC1/BMP5/AR/EGFR/WNT5A/APLNR/FGF7/BAD	4

1. BP – Biological Process, CC – Cellular Component, MF – Molecular Function
2. Grey shading indicates terms related to matrix.
3. Bold and underlined indicates genes that are in the top 20 dysfunction genes in Table 2

Table 3 shows gene ontology (GO) terms associated with the top 200 genes with *decreased* expression in hearts with dysfunction. Eight were associated with matrix remodeling. The pathways included many of the top dysfunction genes, for example, *FBLN1*, *ADAMTSL3*, *DCN*, and *PTN*. As an internal control, and because of the clinical role of BNP blood levels, we included the gene for BNP (*NPPB*), which was significantly increased in hearts with dysfunction.

Table S6 shows GO terms associated with the 200 genes with the most significantly *increased* expression in dysfunction. These terms reflect TCMR-like inflammation, including genes increased in TCMR such as *CTLA4, CD8A, CD8B*, and IFNG-inducible genes such as *ICOS* and HLA genes. Arginase 2 (*ARG2*), a top survival gene (see below), was also associated with some dysfunction pathways. IGFBP2, one of the top 4 genes increased in hearts with dysfunction, appeared in several GO terms associated with inflammation and immune response.

Dysfunction classifier

Figure 2A shows the AUC = 0.73 for the ROC curve for the dysfunction classifier ($LoLVEF_{Prob}$). Figure 2B plots the dysfunction classifier score ($LoLVEF_{Prob}$) against recorded LVEF. Most hearts with LVEF > 55 had low dysfunction classifier scores. Hearts with LVEF ≤ 55 usually had high classifier scores.

The dysfunction classifier correlated with the recorded LVEF, with Spearman correlation coefficient (SCC) of –0.29 ($p < 2.2E{-}16$) in all hearts. The correlations were stronger in hearts with LVEF ≤ 55 (SCC = –0.39, $p = 3.9E{-}09$) than in hearts with LVEF > 55 (SCC = –0.07, $p = 0.04$). Thus, the dysfunction-related molecular changes were present in some hearts with LVEF > 55 but not correlated with LVEF in those hearts.

Genes associated with survival

There were 1,181 biopsies with available follow-up times > 0 days, documented graft status, and TxBx > 0 days, and survival analysis was based on 1 random biopsy per transplant—779 cases with 74 failures by 3 years post-biopsy—53 of which occurred before 1 year. The median follow-up time postbiopsy was 313 days (range 1-3,854 days, Table 1).

Cox regression identified genes most differentially expressed in 74/779 hearts that failed within 3 years post-biopsy (Table 4). Of the top 20 genes sorted by *p*-value, 15 had decreased expression and 5 had increased expression in hearts that failed.

The top genes decreased in hearts that failed included matrix-related genes—*SMOC2*, *ECM2*, *LUM*, *PTN*, and *ADAMTSL3*. Other decreased genes—*LAMA4*, *ALDH1A2*, *LHFP*, and *RGS5*—were highly expressed in endothelial cells (HUVECs in our cell panel).

The top 2 increased genes in hearts that failed were *ARG2* and enolase 2 (*ENO2*). Although not in the top 20, endothelin 1 (EDN1) and BNP (*NPPB*) were also increased in failing hearts.

Three top survival genes overlapped with top dysfunction genes: *ENO2* (increased in hearts that failed and hearts with dysfunction) and *PTN* and *ADAMTSL3* (decreased in hearts that failed and hearts with dysfunction).

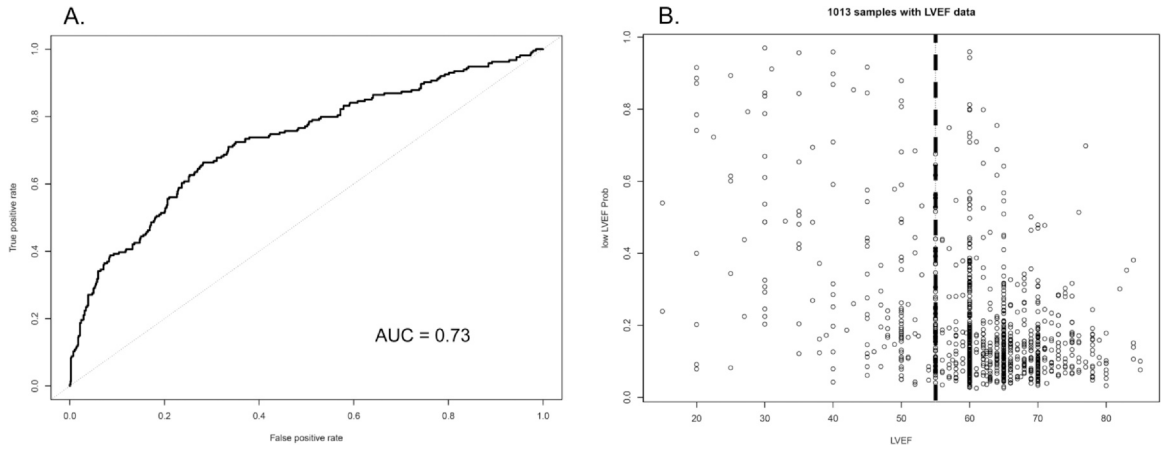

Figure 2 Characteristics of the dysfunction classifier ($LoLVEF_{Prob}$). (A) The ROC curve for the dysfunction classifier ($LoLVEF_{Prob}$, AUC = 0.73) (y axis) plotted against the actual LVEF (x axis). (B) Plotting the dysfunction classifier ($LoLVEF_{Prob}$) score (y axis) against the actual LVEF recorded (x axis). Most hearts with LVEF > 55 had low dysfunction classifier scores. Hearts with low LVEF usually had high classifier scores. The Spearman correlation of the classifier with recorded LVEF was: Spearman correlation coefficient (SCC) = –0.29 ($p < 2.2E{-}16$) in all hearts; SCC = –0.39 ($p = 3.9e{-}09$) in hearts with LVEF ≤ 55; and SCC = –0.07 ($p = 0.04$) in hearts with LVEF > 55. LVEF, left ventricular ejection fraction.

Table 4 Top 20 Unique Genes Associated With Graft Survival in Cox Regression Analyses ($N = 779$ EMBs With 74 Postbiopsy Failures Within 3 Years)

Gene Symbol[1]	Gene Name	PBT	P-value (3 yr)	HR 3yr	Mean Failures 3yr	Mean Censor 3yr
ARG2	arginase 2	IRITD3	**4.0E-21**	**0.728**	**38**	**23**
ENO2	enolase 2 (gamma, neuronal)		**2.8E-19**	**1.551**	**204**	**157**
SMOC2	SPARC related modular calcium binding 2	IRITD5	1.9E-17	-0.731	353	563
ALDH1A2	aldehyde dehydrogenase 1 family, member A2	cIRIT	3.1E-17	-0.734	97	182
PDE5A	phosphodiesterase 5A, cGMP-specific		3.7E-16	-1.14	235	355
LHFP	lipoma HMGIC fusion partner	IRITD3	5.2E-16	-1.349	1406	1810
SCN4B	sodium channel, voltage gated, type IV beta subunit	KT1	7E-16	-0.974	102	157
ECM2	extracellular matrix protein 2, female organ/adipocyte specific		9.3E-16	-0.938	258	402
LUM	lumican	IRITD5	1.1E-15	-0.485	1183	2252
PTN	pleiotrophin		3.1E-15	-0.666	286	539
TRIL	TLR4 interactor with leucine-rich repeats	KT1	4.1E-15	-1.263	35	56
KITLG	KIT ligand		4.7E-15	-1.317	362	497
ERO1A	endoplasmic reticulum oxidoreductase alpha	cIRIT	**8.4E-15**	**1.439**	**190**	**157**
ADAMTSL3	ADAMTS like 3		**1.2E-14**	**-0.918**	**79**	**124**
SLC2A1	solute carrier family 2 (facilitated glucose transporter), member 1	cIRIT	**2.2E-14**	**1.456**	**458**	**363**
APLNR	apelin receptor	KT1	2.5E-14	-0.872	245	402
LAMA4	laminin, alpha 4		3.0E-14	-0.944	571	727
AATF	apoptosis antagonizing transcription factor		**3.5E-14**	**3.534**	**260**	**236**
FNDC1	fibronectin type III domain containing 1		3.7E-14	-0.687	108	207
RGS5	regulator of G-protein signaling 5	KT1	3.7E-14	-0.538	1688	2818
Selected relevant genes not present in the top 20						
NPPB	natriuretic peptide B		4.0E-05	0.2	3164	1353
EDN1	endothelin 1	ENDAT, IRITD3	1.4E-12	0.964	138	103

1. Grey shading indicates genes increased in hearts that failed.
Bolding indicates P-values, hazard ratios, mean expression in heart transplants that failured, and mean expression in heart transplants that were censored at 3 years for genes increased in hearts that failed.
Abbreviations: IRITD3 – injury-repair induced transcripts day 3, IRITD5 - injury-repair induced transcripts day 5, MCAT- mast cell transcripts, cIRIT- cardiac injury and repair transcripts, ENDAT – endothelial transcripts, KT1 – kidney transcripts

Table 5 shows the GO categories overrepresented by the top 200 genes *decreased* in hearts that failed, with 11 related to extracellular matrix structural constituents or basement membrane.

Table S7 shows the GO categories overrepresented by the top 200 genes *increased* in hearts that failed: 4 related to response to hypoxia and reactive oxygen species and 4 related to glycolysis (all including *ENO2*). Endothelin 1 (EDN1) was associated with 7/20 survival-related GO categories.

Survival classifiers

We used the survival data set to build two types of classifiers for predicting 3-year postbiopsy survival.

The RF classifier was given 33 previously published variables, including 2 clinical variables (time posttransplant and indication vs protocol status). Figure 3A shows the relative importance of the 33 features. Figure 3B shows a trimmed RF model using the selected top 8 variables (see Methods). Note that the relative

Table 5 GO Terms Associated With the Top 200 Unique Survival Genes That Are Decreased in Hearts That Failed ($N = 779$ EMBs With 74 Postbiopsy Failures Within 3 Years)

ONTOLOGY[1]	ID	Description[2]	P value	Q value	Gene ID[3]	Count
CC	GO:0062023	collagen-containing extracellular matrix	1.65E-16	3.55E-14	***SMOC2***/***ECM2***/***LUM***/***LAMA4***/***DCN***/COL15A1/OGN/COL6A6/ASPN/EGFLAM/ITIH5/ MATN2/LAMC1/CXCL12/FREM1/SPARC/LEFTY2/EMILIN3/LTBP4/DPT/TGFB3/ ***FBLN1***/LAMB3/VIT/CILP/COL4A4/COL9A1/TNXA/THBS4	29
MF	GO:0005201	extracellular matrix structural constituent	3.18E-15	8.83E-13	***LUM***/***LAMA4***/***DCN***/COL15A1/OGN/COL6A6/ANOS1/ASPN/MATN2/LAMC1/SPARC/ EMILIN3/LTBP4/DPT/***FBLN1***/LAMB3/CILP/COL4A4/COL9A1	19
CC	GO:0005604	basement membrane	1.32E-10	1.42E-08	***SMOC2***/***LAMA4***/COL15A1/***EGFLAM***/LAMC1/FREM1/SPARC/***FBLN1***/LAMB3/ COL4A4/COL9A1/THBS4	12
BP	GO:0030198	extracellular matrix organization	8.92E-10	7.38E-07	***SMOC2***/***ECM2***/LUM/***ADAMTSL3***/COL15A1/TLL2/COL6A6/EGFLAM/LAMC1/TCF15/DPT/ ***FBLN1***/LAMB3/VIT/COL4A4/COL9A1/TNXA/DDR2	18
BP	GO:0043062	extracellular structure organization	9.40E-10	7.38E-07	***SMOC2***/***ECM2***/***LUM***/***ADAMTSL3***/COL15A1/TLL2/COL6A6/EGFLAM/LAMC1/TCF15/DPT/ ***FBLN1***/LAMB3/VIT/COL4A4/COL9A1/TNXA/DDR2	18
BP	GO:0045229	external encapsulating structure organization	1.04E-09	7.38E-07	***SMOC2***/***ECM2***/***LUM***/***ADAMTSL3***/COL15A1/TLL2/COL6A6/EGFLAM/LAMC1/TCF15/DPT/ ***FBLN1***/LAMB3/VIT/COL4A4/COL9A1/TNXA/DDR2	18
BP	GO:0060485	mesenchyme development	1.19E-06	6.33E-04	ALDH1A2/***KITLG***/APLNR/EPHA3/SEMA6A/BMP5/PDGFRB/FRZB/NRP1/TCF15/IL17RD/ MEOX1/SEMA6D/TGFB3	14
CC	GO:0005581	collagen trimer	1.88E-06	1.34E-04	***LUM***/COL15A1/COL6A6/C1QTNF9/C1QTNF7/C1QTNF9B/COL4A4/ COL9A1	8
BP	GO:0038084	vascular endothelial growth factor signaling pathway	7.69E-06	3.27E-03	***SMOC2***/***DCN***/SEMA6A/ADGRA2/PDGFRB/NRP1	6
MF	GO:0008083	growth factor activity	2.40E-05	3.33E-03	***PTN***/***KITLG***/OGN/BMP5/CXCL12/LEFTY2/NTF3/TGFB3/ THBS4	9
MF	GO:0005518	collagen binding	4.41E-05	3.43E-03	***ECM2***/***LUM***/***DCN***/ASPN/SPARC/DDR2	6
BP	GO:0031589	cell-substrate adhesion	4.80E-05	1.70E-02	***ECM2***/EPHA3/***EGFLAM***/ATP1B2/DLC1/LAMC1/FREM1/SGCE/NRP1/ ***FBLN1***/LAMB3/VIT/TTYH1	13
MF	GO:0030021	extracellular matrix structural constituent conferring compression resistance	4.94E-05	3.43E-03	***LUM***/***DCN***/OGN/ASPN	4
BP	GO:0050920	regulation of chemotaxis	6.12E-05	1.86E-02	***SMOC2***/***PTN***/SEMA6A/ADGRA2/PDGFRB/CXCL12/NRP1/NTF3/ SEMA6D/THBS4	10
BP	GO:0035924	cellular response to vascular endothelial growth factor stimulus	7.42E-05	1.97E-02	***SMOC2***/***DCN***/SEMA6A/ADGRA2/PDGFRB/NRP1	6
MF	GO:0005539	glycosaminoglycan binding	7.95E-05	4.42E-03	***SMOC2***/***ECM2***/***PTN***/***DCN***/ANOS1/***EGFLAM***/NRP1/LTBP4/VIT/ THBS4	10
MF	GO:0140359	ABC-type transporter activity	9.70E-05	4.49E-03	***ABCA9***/***ABCA8***/***ABCA6***/ABCA10/ABCC9	5
BP	GO:1900746	regulation of vascular endothelial growth factor signaling pathway	1.18E-04	2.33E-02	***SMOC2***/***DCN***/SEMA6A/ADGRA2	4
BP	GO:0048762	mesenchymal cell differentiation	1.20E-04	2.33E-02	ALDH1A2/***KITLG***/EPHA3/SEMA6A/BMP5/FRZB/NRP1/IL17RD/ SEMA6D/TGFB3	10
BP	GO:0045765	regulation of angiogenesis	1.21E-04	2.33E-02	***SMOC2***/APLNR/***DCN***/SEMA6A/RHOJ/ADGRA2/SPARC/NRP1/***AMOT***/ ADGRB3/ISM1/THBS4	12

1. BP – Biological Process, CC – Cellular Component, MF – Molecular Function
2. Shading indicates terms related to VEGF or angiogenesis.
3. Bold and underlined indicates genes that are in the top 20 dysfunction genes in Table 2 or survival genes in Table 4

importance does not indicate the direction of the effect of the variable. The top four variables were biopsy indication (indication versus protocol), scores for the dysfunction classifier (LoL-VEF_{Prob}), mast cell transcripts (MCAT), and immunoglobulin transcripts (IGT). The ordering in the trimmed model was similar to the top of the 33-feature model. The only clinical variable used in the trimmed RF model was indication status.

The glmnet classifier was gene-based, using lasso regression to select a limited number of probes sets from the 12,500 interquartile range-filtered probe sets it was given as inputs. The predictive value of the glmnet classifier (C-statistic = 0.773 from the combined OOB predicted scores) was similar to that of the trimmed RF model (0.779, same OOB biopsies evaluated). No clinical variables were used in the glmnet model.

The added predictive value of the 7 molecular variables used in Figure 3B is highly significant. Using Cox regression analysis, the likelihood ratio test p-value assessing the significance of the added value of the 7 molecular variables to biopsy indication alone is $p = 4.4E{-}16$. Adding the 7 molecular variables to a model with biopsy indication and measured LVEF is $p = 4.3E{-}7$.

Combining both classifiers to create a survival score

We used the mean of the RF and glmnet classifiers as the survival score for each biopsy. Figure 3C and D shows Kaplan-Meier plots for the survival scores when biopsies were divided into quintiles. The mean score strongly correlated with risk for survival in the OOB biopsies: the lowest survival quintile had mean survival estimates of 50% versus >95% for the highest quintile. Graft loss within one year was concentrated in the lowest quintile. The numbers of biopsies at risk per time period are tallied in the table below each panel.

The best survival predictions (based on concordance) were with the survival score based on the combination (mean) of the RF and glmnet scores for each biopsy (Table S8).

Relating the dysfunction score and the survival probability score to other rejection and injury scores in 3,230 biopsies

We evaluated the correlation between previously annotated molecular rejection and injury transcript set scores and the dysfunction and survival classifier scores in the complete set of 3,230 biopsies. We calculated the SCC of the dysfunction classifier score and the survival probability classifier scores with the rejection archetype scores and various transcript sets (Table 6).

The TCMR archetype score, macrophage score, cardiac injury score, and the atrophy-fibrosis score correlated with increased dysfunction scores and decreased survival probability.

The ABMR archetype score and related transcript sets had minimal correlations with dysfunction scores but strong positive correlations with survival probability.

Normal heart transcripts (HTs) are correlated with lower dysfunction scores and higher survival probability. The dysfunction classifier score was strongly correlated with decreased

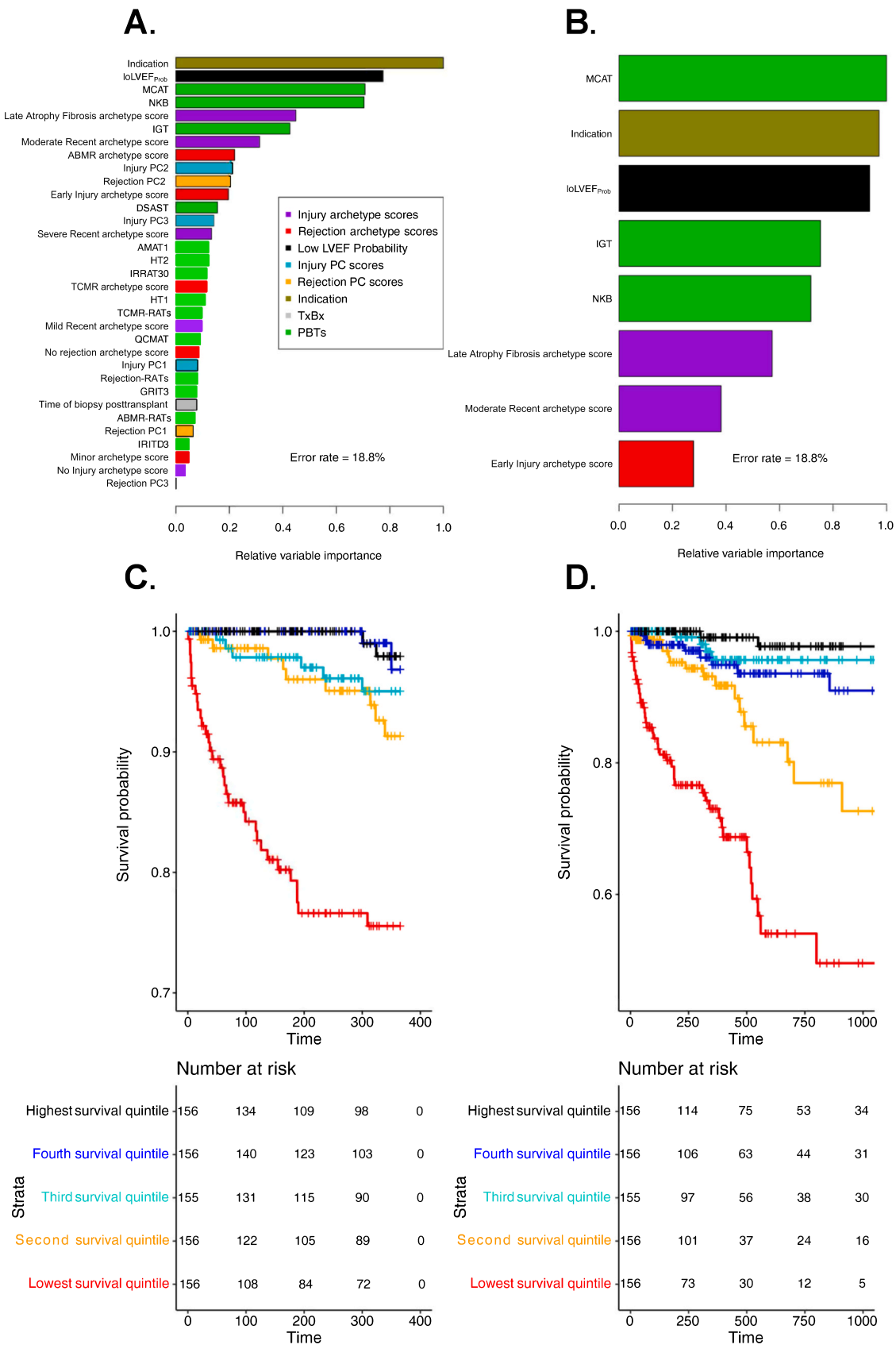

(caption on next page)

Figure 3 Models predicting the survival of heart transplants after biopsy. (A) 33-variable random forest model, showing the relative importance of each of the 33 variables given to the RF model. Relative importance does not indicate the direction of the effect of these variables. (B) The trimmed RF model using only 8 top variables from the 33 variable model. The 8 variables were selected based on the minimal depth method using the "var.select" function. (C-D) Kaplan-Meier plots for the survival scores using the survival probability score: the mean of the RF and glmnet classifier scores. The scores for each biopsy were used to divide the biopsies into quintiles. All scores are those assigned to out-of-bag biopsies. The lowest survival quintile had mean survival estimates of only 50% by 3 years postbiopsy, whereas the highest had greater than 95% survival. ABMR-RATs, antibody-mediated rejection-associated transcript set; AMAT1, alternatively activated macrophage transcript set; DSAST, donor-specific antibody-selective transcripts; HT1 and HT2, heart transcripts set 1 and set 2; IGT, immunoglobulin transcripts; IRITD3, injury and repair-induced transcripts, day 3; IGT, immunoglobulin transcripts; IRRAT30, injury and repair-associated transcripts; loLVEFprob, low left ventricular ejection fraction probability classifier; LVEF, left ventricular ejection fraction; MCAT, mast cell transcripts; PC, principal component; TCMR-RATs, T cell-mediated rejection-associated transcripts.

Table 6 Spearman Correlation Coefficients (SCC) Showing the Relationship Between Transcript Set Scores (PBTs) With the Dysfunction Probability Classifier Score ($LoLVEF_{Prob}$) and the Heart 3-Year Postbiopsy Survival Probability in All Biopsies ($N = 3,230$).

Molecular feature category	Abbreviation	SCC between features and $LoLVEF_{Prob}$ (N=3230)		SCC between features and 3-year survival probability (N=3230)	
		SCC[1]	P-value	SCC[1]	P-value
TCMR-related	TCMR archetype score	**0.34**	**<2.2E-16**	-0.10	1.9E-09
ABMR-related	ABMR archetype score	0.14	4.1E-15	0.23	<2.2E-16
	DSAST	0.06	0.0015	**0.35**	**1.2E-93**
	NKB	0.09	9.9E-07	**0.40**	**4.8E-130**
Macrophage-related	AMAT1	**0.39**	**1.1E-117**	-0.17	9.5E-22
Recent injury	Cardiac injury (cIRIT)	**0.38**	**4.9E-111**	-0.16	8.0E-20
Atrophy-fibrosis	IGT	**0.30**	**2.2E-68**	-0.13	6.9E-13
Normal heart transcripts	HT1 (except SLCs)	**-0.57**	**3.5E-275**	0.26	**8.6E-50**
	HT2 (SLCs)	**-0.63**	**3.5E-275**	**0.34**	**5.6E-87**
Time posttransplant		0.14	8.7E-16	0.09	1.1E-07

1. Shaded indicates variables that correlate both with increased dysfunction and decreased survival probability. Bold indicates SCC≥ (+0.3) or ≤(-0.3)

expression of those transcripts expressed in normal hearts, particularly the solute carriers (HT2) with SCC = –0.63. The survival probability classifier correlated negatively with expression of the HTs. Thus, dedifferentiation plays a major role in dysfunction and a significant role in predicting future graft loss.

Discussion

This study of endomyocardial biopsies (EMBs) defined the molecular features associated with depressed LVEF and reduced postbiopsy survival. Dysfunction, defined as LVEF ≤ 55, correlated most strongly with genes and GO terms associated with decreased expression of many matrix-related genes, plus loss of normal heart transcripts—parenchymal dedifferentiation, accompanied by inflammation. Survival analysis found that short-term failure shared features with dysfunction genes but also included increased expression of genes related to response to hypoxia and glycolysis and reduced expression of genes related to VEGF pathways and angiogenesis. In the expanded set of 3,230 biopsies, dysfunction was strongly associated with decreased expression of normal heart genes such as solute carriers and increased expression of genes related to TCMR, injury, and macrophages. The survival probability classifier correlated with high expression of ABMR-related transcripts as expected[10,12] and normal heart transcripts, and anticorrelated with TCMR, inflammation, and injury transcripts. Expression of the natriuretic peptide B gene (*NPPB*)[33] was strongly associated with dysfunction and graft loss, serving as an internal control, given the strong association of blood BNP levels with dysfunction and failure in cardiology.

The use of LVEF ≤ 55 as the cutoff for dysfunction was to some extent arbitrary but was guided by the desire to have a group with unquestionably good LVEF to compare with a somewhat heterogeneous group that had lower LVEF, as illustrated in Figure 2B. However, based on our unpublished experience and the distribution of values (Figure 2B), the classifier and the conclusions about dysfunction would have been similar regardless of the cutoff selected.

As expected from earlier INTERHEART analyses,[10] ABMR-related molecular changes had little association with dysfunction but were strongly associated with relatively good short-term graft survival. However, ABMR probably poses late risks and we have shown that ABMR is associated with atrophy-fibrosis in late EMBs.[12] It is likely that ABMR slowly increases fibrosis in heart transplants, similar to the findings in

kidney transplants, where short-term survival in early-stage ABMR is good but slow deterioration follows.[34]

The top dysfunction genes and GO pathways were related to matrix (and strongly expressed in fibroblasts per the Human Protein Atlas[35]) but surprisingly were decreased, whereas a priori we would have expected dysfunction to be associated with fibrogenesis. These decreased matrix genes were associated with loss of expression of normal heart genes and some increases in cardiomyocyte genes: for example, regulator of calcineurin 1 (*RCAN1*), which is of interest given the role of calcineurin in cardiac hypertrophy[36-40] and skeletal muscle hypertrophy.[41,42] TCMR, inflammation, injury, and atrophy-fibrosis were also correlated with dysfunction, and presumably indicate the source of some damage to the parenchyma and matrix, but these associations were weaker.

The survival genes and GO pathways offer insights into the role of the microvasculature in hearts at risk, indicating the importance of ARG2, endothelin, and the VEGF and angiogenesis pathways, which in turn may be related to the response to hypoxia and glycolysis pathways. This recalls the microcirculation changes described in hearts with chronic allograft vasculopathy (CAV), with decreased capillary density but increased capillary wall thickness.[43] While TCMR undoubtedly causes extensive damage,[12] the primary association with risk was not related to rejection activity, which reflects parenchymal states that persist after TCMR is treated. ARG2 is a mitochondrial enzyme that degrades L-arginine, the substrate for nitroc oxide synthase (NOS), and thus depresses nitric oxide synthesis. ARG2 is broadly expressed in macrophages, endothelial cells, and cardiomyocytes. *ENO2* is involved in glycolysis and is expressed in cardiomyocytes but is also broadly expressed. In experimental studies, increased ARG2 creates substrate limitation for NOS, leaving uncoupled NOS to produce superoxide anions and contribute to contractile dysfunction.[44] The survival genes and GO pathways also overlapped the dysfunction genes: for example, both dysfunction and survival were related to increased expression of *ENO2*, a regulator of glycolysis.

In RF, expression of MCATs was unexpectedly associated with improved survival; the basis for this is currently under investigation. MCAT expression (particularly *FCER1A*) is increased in heart ABMR, perhaps because MCATs are expressed in NK cells as well as mast cells.

As with all observational studies, the genes described represent associations and correlations with the underlying disease process, and none of the relationships are necessarily causative in nature. Another limitation to this study is the small number of events in the survival analysis, although it is greater (74 versus 52) than in the earlier study.[12,17] We need to continue to examine the long-term determinants of survival in larger studies, such as the ongoing Trifecta-Heart study. We note the interesting change in regulator of calcineurin 1 (RCAN1) expression between patients with high versus low LVEF. However, the limited detail of the available immunosuppression data and the overwhelming use of calcineurin inhibitors in the population made the relationship to calcineurin inhibitors impossible to assess. While single-cell sequencing may present additional results of interest and is now shown to be possible with frozen EMB specimens,[45] it is not suitable for routine diagnostics. Microarrays remain the most suitable and stable technology for our purposes in this study. While no single-cell data is currently available in this study, we are actively incorporating the application of insights gained from single-cell studies in our ongoing analyses.

It will be of interest to pursue the relationship between the dysfunction and survival genes and major features of the late heart transplant population such as CAV and diastolic dysfunction. CAV has a major microcirculation component,[43] and the survival genes were related to reduced expression of genes in the VEGF and angiogenesis pathways and increased ARG2 expression—indicating possible dysfunction in nitric oxide production and increased endothelin expression. Dysfunction-related molecular changes also occurred in some hearts with LVEF > 55, indicating molecular abnormalities in hearts with preserved LVEF, with possible relevance to diastolic dysfunction and the problem of heart failure with preserved ejection fraction.[1]

Authors contributions

PFH: principal investigator, manuscript writing/reviewing. JR, KMT, MM: manuscript writing/reviewing, data analyses. AZA-Z, MC, MGC-L, ECD, MD, JG, DHK, JK, PM, LP, KS, JS, AZ: biopsy collection, manuscript reviewing.

Disclosure statement.

P F Halloran holds shares in Transcriptome Sciences Inc., a University of Alberta research company with an interest in molecular diagnostics; has given lectures for Thermo Fisher and is a consultant for CSL Behring. The other authors have declared that no conflict of interest exists.

Acknowledgments

This research has been principally supported by grants from Genome Canada, Canada Foundation for Innovation, the University of Alberta Hospital Foundation, the Alberta Ministry of Advanced Education and Technology, the Mendez National Institute of Transplantation Foundation, and Industrial Research Assistance Program. Partial support was also provided by funding from a licensing agreement with the 1 Lambda division of Thermo Fisher. Dr Halloran held a Canada Research Chair in Transplant Immunology until 2008 and currently holds the Muttart Chair in Clinical Immunology. Some biopsies were provided by Dr Alexandre Loupy, Paris, France.

Financial support

Funds for this study were derived from Genome Canada, the Canada Foundation for Innovation, from a licensing agreement with Thermo Fisher, from a research grant from Natera.

Supplementary data

Supplementary data associated with this article can be found in the online version at doi:10.1016/j.healun.2023.11.013.

References

1. Vejpongsa P, Torre-Amione G, Marcos-Abdala HG, et al. Long term development of diastolic dysfunction and heart failure with preserved left ventricular ejection fraction in heart transplant recipients. Sci Rep 2022;12:3834.
2. Colvin M, Smith JM, Hadley N, et al. OPTN/SRTR 2018 annual data report: heart. Am J Transpl 2020;20(Suppl s1):340-426.
3. Stehlik J, Kobashigawa J, Hunt SA, Reichenspurner H, Kirklin JK. Honoring 50 years of clinical heart transplantation in circulation: in-depth state-of-the-art review. Circulation 2018;137:71-87.
4. Aleksova N, Alba AC, Molinero VM, et al. Risk prediction models for survival after heart transplantation: a systematic review. Am J Transpl 2020;20:1137-51.
5. Halloran PF, Madill-Thomsen KS, Reeve J. The molecular phenotype of kidney transplants: insights from the MMDx project. Transplantation 2023. https://doi.org/10.1097/TP.0000000000004624. Online ahead of print.
6. Halloran PF, Madill-Thomsen KS. The molecular microscope diagnostic system: assessment of rejection and injury in heart transplant biopsies. Transplantation 2023;107:27-44.
7. Reeve J, Bohmig GA, Eskandary F, et al. Generating automated kidney transplant biopsy reports combining molecular measurements with ensembles of machine learning classifiers. Am J Transpl 2019;19:2719-31.
8. Halloran KM, Parkes MD, Chang J, et al. Molecular diagnosis of rejection phenotypes in lung transplant transbronchial biopsies: initial findings of the INTERLUNG study. J Heart Lung Transplant 2018;37:S80.
9. Parkes M, Halloran K, Famulski K, Halloran P, Grp IS. Molecular phenotypes of injury and rejection in lung transplant transbronchial biopsies. Am J Transplant 2018;18:274-5.
10. Halloran PF, Potena L, Van Huyen JD, et al. Building a tissue-based molecular diagnostic system in heart transplant rejection: the heart Molecular Microscope Diagnostic (MMDx) System. J Heart Lung Transpl 2017;36:1192-200.
11. Halloran PF, Reeve J, Akalin E, et al. Real time central assessment of kidney transplant indication biopsies by microarrays: the INTERCOMEX study. Am J Transpl 2017;17:2851-62.
12. Madill-Thomsen KS, Reeve J, Aliabadi-Zuckermann A, et al. Assessing the relationship between molecular rejection and parenchymal injury in heart transplant biopsies. Transplantation 2022;106:2205-16.
13. Halloran PF, Venner JM, Famulski KS. Comprehensive analysis of transcript changes associated with allograft rejection: combining universal and selective features. Am J Transpl 2017;17:1754-69.
14. Parkes MD, Aliabadi AZ, Cadeiras M, et al. An integrated molecular diagnostic system for rejection and injury in heart transplant biopsies. J Heart Lung Transplant 2019;38:636-46.
15. Halloran PF, Reeve J, Aliabadi AZ, et al. Exploring the cardiac response to injury in heart transplant biopsies. JCI Insight 2018;3:e123674.
16. Madill-Thomsen KS, Bohmig GA, Bromberg J, et al. Relating molecular T cell-mediated rejection activity in kidney transplant biopsies to time and to histologic tubulitis and atrophy-fibrosis. Transplantation 2023;107:1102-14.
17. Halloran PF, Madill-Thomsen KS, Aliabadi-Zuckermann A, et al. Many heart transplant biopsies currently diagnosed as no rejection have mild molecular antibody-mediated rejection-related changes. J Heart Lung Transplant 2021;41:334-44.
18. Halloran PF, Bohmig GA, Bromberg J, et al. Archetypal analysis of injury in kidney transplant biopsies identifies two classes of early AKI. Front Med (Lausanne) 2022;9:817324.
19. Reeve J, Kim DH, Crespo-Leiro MG, et al. Molecular diagnosis of rejection phenotypes in 889 heart transplant biopsies: the INTERHEART study. J Heart Lung Transplant 2018;37:S27.
20. Alberta Transplant Applied Genomics Centre. Gene lists 2019. https://www.ualberta.ca/medicine/institutes-centres-groups/atagc/research/gene-lists.html.
21. Ishwaran H, Kogalur UB. Fast unified random forests for survival, regression, and classification (RF-SRC). R package version 302. Available at: ⟨https://cranr-projectorg/package=randomForestSRC⟩; 2022.
22. Mengel M, Reeve J, Bunnag S, et al. Molecular correlates of scarring in kidney transplants: the emergence of mast cell transcripts. Am J Transpl 2009;9:169-78.
23. Famulski KS, de Freitas DG, Kreepala C, et al. Molecular phenotypes of acute kidney injury in kidney transplants. J Am Soc Nephrol 2012;23:948-58.
24. Famulski KS, Broderick G, Einecke G, et al. Transcriptome analysis reveals heterogeneity in the injury response of kidney transplants. Am J Transpl 2007;7:2483-95.
25. Famulski KS, Einecke G, Sis B, et al. Defining the canonical form of T-cell-mediated rejection in human kidney transplants. Am J Transpl 2010;10:810-20.
26. Hidalgo LG, Sis B, Sellares J, et al. NK cell transcripts and NK cells in kidney biopsies from patients with donor-specific antibodies: evidence for NK cell involvement in antibody-mediated rejection. Am J Transpl 2010;10:1812-22.
27. Einecke G, Reeve J, Mengel M, et al. Expression of B cell and immunoglobulin transcripts is a feature of inflammation in late allografts. Am J Transplant 2008;8:1434-43.
28. Hidalgo LG, Sellares J, Sis B, Mengel M, Chang J, Halloran PF. Interpreting NK cell transcripts versus T cell transcripts in renal transplant biopsies. Am J Transpl 2012;12:1180-91.
29. Halloran PF, de Freitas DG, Einecke G, et al. The molecular phenotype of kidney transplants. Am J Transpl 2010;10:2215-22.
30. Friedman J, Hastie T, Tibshirani R. Regularization paths for generalized linear models via coordinate descent. J Stat Softw 2010;33:22.
31. Ritchie ME, Phipson B, Wu D, et al. limma powers differential expression analyses for RNA-sequencing and microarray studies. Nucleic Acids Res 2015;43:e47.
32. Therneau T. A package for survival analysis in R_. R package version 32-7. Available at: ⟨https://CRANR-projectorg/package=survival⟩; 2020.
33. Dickstein K. Natriuretic peptides in detection of heart failure. Lancet 1998;351:4.
34. Einecke G, Reeve J, Gupta G, et al. Factors associated with kidney graft survival in pure antibody-mediated rejection at the time of indication biopsy: importance of parenchymal injury but not disease activity. Am J Transpl 2021;21:1391-401.
35. Uhlen M, Fagerberg L, Hallstrom BM, et al. Proteomics. Tissue-based map of the human proteome. Science 2015;347:1260419.
36. Luo Z, Shyu K-G, Gualberto A, Walsh K. Calcineurin inhibitors and cardiac hypertrophy. Nat Med 1998;4:1092-3.
37. Mokentin JD, Lu J-R, Antos CL, et al. A calcineurin-dependent transcriptional pathway for cardiac hypertrophy. Cell 1998;93:215-28.
38. OIson EN, Molkentin JD. Prevention of cardiac hypertrophy by calcineurin inhibition. Hope or hype? Circ Res 1999;84:623-32.
39. Sugden PH. Signaling in mycocardial hypertrophy. Life after calcineurin? Circ Res 1999;84:633-46.
40. Walsh RA. Calcineurin inhibition as therapy for cardiac hypertrophy and heart failure. Requiescat in pace? Circ Res 1999;84:741-3.
41. Semsarian C, Wu M-J, Ju Y-K, et al. Skeletal muscle hypertrophy is mediated by a Ca^{2+}-dependent calcineurin signalling pathway. Nature 1999;400:576-80.
42. Musarò A, McCullagh KJA, Naya FJ, Olson EN, Rosenthal N. IGF-1 induces skeletal myocyte hypertrophy through calcineurin in association with GATA-2 and NF-ATc1. Nature 1999;400:581.
43. Daud A, Xu D, Revelo MP, et al. Microvascular loss and diastolic dysfunction in severe symptomatic cardiac allograft vasculopathy. Circ Heart Fail 2018;11:e004759.
44. Heusch P, Aker S, Boengler K, et al. Increased inducible nitric oxide synthase and arginase II expression in heart failure: no net nitrite/nitrate production and protein S-nitrosylation. Am J Physiol Heart Circ Physiol 2010;299:H446-53.
45. Amancherla K, Qin J, Hulke ML, et al. Single-nuclear RNA sequencing of endomyocardial biopsies identifies persistence of donor-recipient chimerism with distinct signatures in severe cardiac allograft vasculopathy. Circ Heart Fail 2023;16:e010119.